Energies **2015**, *8*, 5555-5576; doi:10.3390/en8065555

OPEN ACCESS

energies

ISSN 1996-1073

www.mdpi.com/journal/energies

Article

Research on a Novel Power Inductor-Based Bidirectional Lossless Equalization Circuit for Series-Connected Battery Packs

Xiangwei Guo [1,2,*], Longyun Kang [1,2], Zhizhen Huang [1,2], Yuan Yao [1,2] and Huizhou Yang [3]

[1] New Energy Research Center of Electric Power College, South China University of Technology, Guangzhou 510640, China; E-Mails: lykang@scut.edu.cn (L.K.); hzz465288@yahoo.com (Z.H.); HeinzYao@outlook.com (Y.Y.)

[2] Guangdong Key Laboratory of Clean Energy Technology, South China University of Technology, Guangzhou 510640, China

[3] Huawei Technologies Co., Ltd., Shenzhen 518129, China; E-Mail: young_scut@126.com

* Author to whom correspondence should be addressed; E-Mail: gxw8611@163.com; Tel.: +86-186-0391-2411.

Academic Editor: K. T. Chau

Received: 2 April 2015 / Accepted: 2 June 2015 / Published: 9 June 2015

Abstract: Cell balancing plays an important role in preserving the life of series-connected battery packs; without a suitable balancing system, the individual cell voltages will differ over time, and the battery pack capacity will decrease quickly. This paper presents a novel power inductor-based bidirectional lossless equalization circuit. This circuit consists of several balancing sub-circuits, which allow the dynamic adjustment of the equalization path and equalization threshold. The simulation and experiment results demonstrate that the proposed circuit, which features a simple control method, fast balancing, and a large equalization current, exhibits outstanding equalization performance.

Keywords: series-connected battery pack; bidirectional lossless equalization; power inductor

1. Introduction

Power batteries require a variety of series or parallel combinations to achieve the voltages or capacities required for various applications. This paper focuses on lithium-ion (Li-ion) battery cells because of their great potential for future vehicle applications [1]. Due to the inhomogeneity among individual cells, subjecting a power battery group to several charging or discharging cycles can cause some of the cells to overcharge or overdischarge during use, which can degrade the group performance, shorten its lifetime, and even pose a safety hazard. To prolong the battery group lifetime, power battery equalization must be realized [2–7].

Depending on the energy transfer mode, equalization circuits can be divided into two types: balancing circuits, which include energy dissipation, and other circuits without energy dissipation [8]. Although several topological structures exist for the latter type, almost all of them use energy storage elements and balancing bypass to build the energy transport channels and directly or indirectly transfer the energy from the high-energy cell to the lower-energy cell or cells. These latter circuits can generally be categorized as either capacitance, converter or transformer circuits, each of which has its own advantages and disadvantages in terms of accuracy, cost, and efficiency. Uno [2], Kim [3], Kobzev [9] and others have proposed several equalization circuit topologies based on switch capacitance, which charges or discharges capacitors to realize energy transfer. However, these circuits suffer from a longer balancing time, especially in cases with a small difference in battery voltage. Converter-type equalization circuits use power inductors for energy transfer and are based on buck, boost or Ćuk converters. The equalization circuits proposed by Lee [4], Yarlagadda [5], Kim [10], Lu [11], Chen [12], and Hou [13] belong to this type. Converter equalization circuits can realize bidirectional energy flow and offer higher balancing efficiency, but often require a complex switch array and a precise control algorithm. Finally, transformer-type equalization circuits have the basic structure of a fly-back transformer [14–17], which can be divided into a variety of types, such as single magnetic cores, multiple magnetic cores, single vice sides, and multiple vice sides. Transformer-type equalization circuits have a high level of integration and high balancing speed but poor expandability and large transformer magnetic flux leakage.

Considering the advantages and disadvantages of the power battery equalization circuits discussed above, this paper proposes a novel power inductor-based equalization circuit with the advantages of a simple structure, a simple control algorithm and high efficiency. The main idea of the equalization circuit is to reduce the charging current of the single cell with a higher terminal voltage and then prevent overcharge during charging by controlling the balancing sub-circuits. During discharge, the proposed equalization circuit can reduce the discharging current of the low-voltage single cell and then prevent over-discharge by controlling the balancing sub-circuits. In the suspended state, the equalization circuit can realize cell discharging with high energy and cell charging with low energy.

The remainder of this paper is organized as follows: in Section 2, the structure and principle of equalization circuits are described. In Section 3, the fundamental parameters of the equalization circuit are calculated. The simulation framework is introduced in Section 4. The experimental verifications are presented in Section 5. Finally, conclusions are given in Section 6.

2. Equalization Circuit Structure and Principles

In this section, the equalization circuit structure and principles are described. The equalization principles include the single-cell equalization principle and two fluctuating battery parts equalization principle.

2.1. Equalization Circuit Structure

The equalization circuit diagram is shown in Figure 1, where Figure 1a is the equalization circuit schematic diagram and Figure 1b is the balancing sub-circuit principle diagram. A battery pack with cutoff point K is divided into two parts. The total number of cells can be odd or even. If n is an even number, $n = 2 \times k$; if n is an odd number, $n = 2 \times k - 1$.

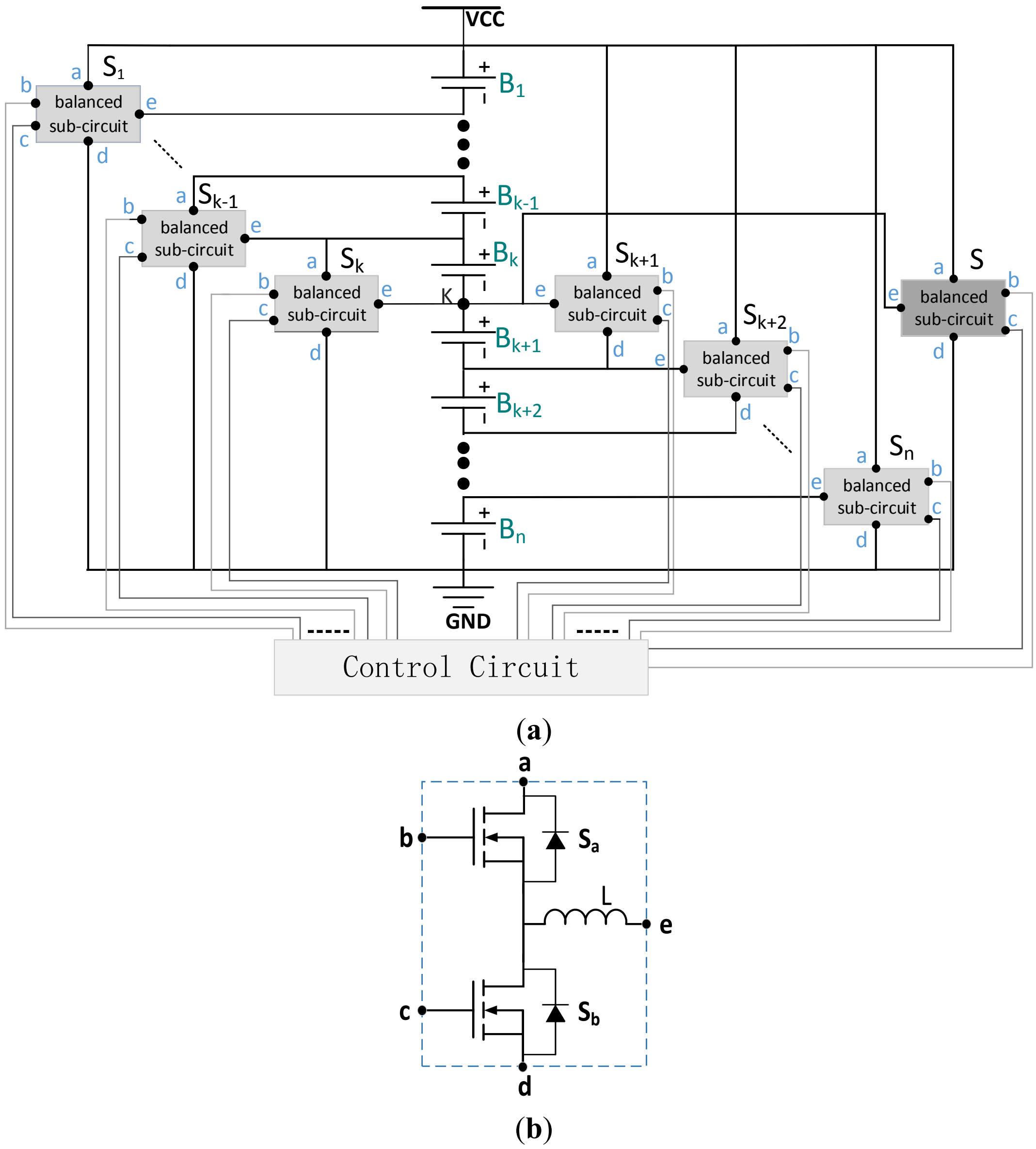

Figure 1. Equalization circuit. (**a**) Equalization circuit scheme; (**b**) Balancing sub-circuit scheme.

In this process, the battery pack has four different working conditions: charging, discharging, the suspended state after charging, and the suspended state after discharging. Among these working conditions, the equalization principles of the charging state and the suspended state after charging are consistent, and the equalization principle of the discharging state is the same as that of the suspended state after discharging. The novelty of the proposed circuit is in the dynamic adjustment of the equalization path and of the equalization threshold, described as follows:

(1) Dynamic adjustment of the equalization path. During equalization, the balancing sub-circuit S is responsible for the equalization path of the two parts of the battery pack, and the balancing sub-circuit S_i controls the equalization path of single cell B_i.

(2) Dynamic adjustment of the equalization threshold. The equalization circuit has two equalization thresholds; one for the individual cells and one for the two fluctuation parts. If the two equalization thresholds are not met, the equalization circuit stops working.

The balancing sub-circuit S is responsible for balancing the two parts of the battery pack, and its working condition is:

$$\left\| \frac{V_1 + V_2 + \cdots + V_k}{k} \right| - \left| \frac{V_{k+1} + V_{k+2} + \cdots + V_n}{n-k} \right\| > 5\text{mV} \tag{1}$$

Each cell B_i is equipped with a balancing sub-circuit S_i that controls the equalization of the single cell B_i. During charging or within the suspended state after charging, the working condition of S_i is $V_i = V_{\max} > V_{\text{avg}} + 10$ mV; $i = 1,2,\ldots n$; $V_{\text{avg}} = (V_1 + V_2 + \ldots + V_n)/n$. Meanwhile, during discharging or within the suspended state after discharging, the working condition of S_i is $V_i = V_{\min} < V_{\text{avg}} - 10$ mV.

Cell balancing based on voltage uniformity is more easily implemented and more common [18]. In this paper, the single-cell terminal voltage serves as the index of inconsistency.

2.2. Equalization Principle

This paper uses four cells in a series battery pack as an example to elaborate the circuit equalization principle. The equalization circuit is shown in Figure 2. If the inconsistency between single cell B_i and the other cells satisfies the equalization conditions, balancing sub-circuit S_i works. If the two fluctuation parts satisfy the working conditions of balancing sub-circuit S, circuit S works. Finally, the equalization process is over when neither S_i nor S works.

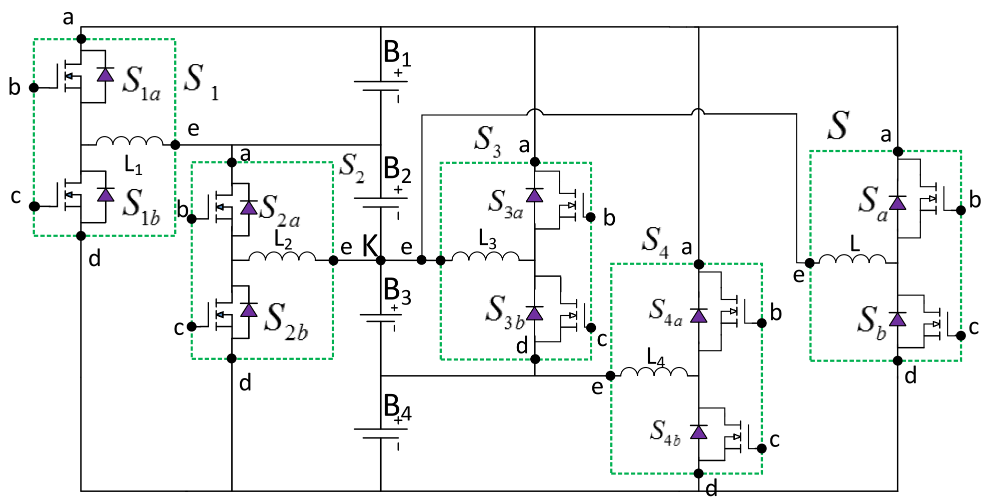

Figure 2. Equalization circuit of four series-connected cells.

2.2.1. Single-Cell Equalization Principle

(1) Equalization principles for the charging process or the suspended state after charging

The equalization principles of the charging state and suspended state after charging are consistent and involve realizing the equalization by first identifying the higher cell voltage and then controlling the corresponding balancing sub-circuits S_i and S. Suppose that the cell voltage of B_1 is higher than that of the other cells during charging or in the suspended state after charging. The equalization principle can then be divided into the following two main stages:

Stage 1: L_1 charges.

Figure 3 presents a schematic of the equalization principle assuming that the voltage of cell B_1 is higher than that of the other cells during charging or in the suspended state after charging. By closing switch S_{1a}, cell B_1 charges inductor L_1, and L_1 stores energy. The current i_L gradually increases, and some of the electrical energy transfers into magnetic energy stored in the inductor. The closing time t_{on} of switch S_{1a} determines the maximum I_{max} of inductor current i_L:

$$V_{B1} = R_{on} i_L + L\frac{di}{dt} \qquad 0 < t \le t_{on} \tag{2}$$

here, R_{on} is the circuit total resistance when closing switch S_{1a}, including the PCB line resistance, the DC resistance of inductor L_1, and the turn-on resistance of switch S_{1a}. L represents the L_1 inductance, i_L is the current flowing in the inductor, and t_{on} is the closing time of switch S_{1a}.

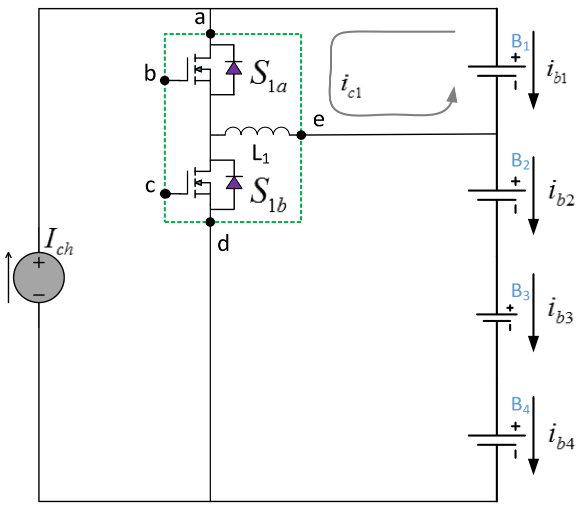

Figure 3. L_1 charging schematic.

A general solution of Equation (2) is:

$$i_L = \frac{V_{B1}}{R_{on}} - \frac{V_{B1}}{R_{on}} e^{-t\frac{R_{on}}{L}} = \frac{V_{B1}}{R_{on}}(1 - e^{-t\frac{R_{on}}{L}}) \qquad 0 < t \le t_{on} \tag{3}$$

If $t = t_{on}$, the circuit current reaches its maximum value; that is:

$$i_L = i_p = \frac{V_{B1}}{R_{on}}(1 - e^{-t_{on}\frac{R_{on}}{L}}) \qquad t = t_{on} \tag{4}$$

In this process, inductor L_1 stores energy, and balancing sub-circuit S_1 decreases the charging current of cell B_1 by absorbing it:

$$i_{\mathrm{B1}} = I_{\mathrm{ch}} - i_{\mathrm{c1}} \tag{5}$$

Stage 2: L_1 discharges.

Figure 4 presents a schematic of the L_1 discharge process. When $t > t_{\mathrm{on}}$, switch $S_{1\mathrm{a}}$ disconnects, and inductor L_1 charges the residual cells through the flywheel diode of switch $S_{1\mathrm{b}}$ to realize the energy transfer from cell B_1 to the other cells. The circuit is the first-order full response, and its solution is:

$$i_{\mathrm{L}} = i_{\mathrm{p}} e^{-(t-t_{\mathrm{on}})\frac{R_{\mathrm{off}}}{L}} - \frac{V_{\mathrm{B}} + V_{\mathrm{D}}}{R_{\mathrm{off}}}\left(1 - e^{-(t-t_{\mathrm{on}})\frac{R_{\mathrm{off}}}{L}}\right) \qquad t_{\mathrm{on}} < t \le t_{\mathrm{d}} \tag{6}$$

where V_{D} is the voltage drop of body diode $S_{1\mathrm{b}}$; R_{off} represents the total resistance of the discharge loop; V_{B} is the total voltage drop of B_2, B_3, and B_4; and t_{d} is the discharge period. Hence, the above formula can also be written as:

$$i_{\mathrm{L}} = \left(i_{\mathrm{p}} + \frac{V_{\mathrm{B}} + V_{\mathrm{D}}}{R_{\mathrm{off}}}\right) e^{-(t-t_{\mathrm{on}})\frac{R_{\mathrm{off}}}{L}} - \frac{V_{\mathrm{B}} + V_{\mathrm{D}}}{R_{\mathrm{off}}} \qquad t_{\mathrm{on}} < t \le t_{\mathrm{d}} \tag{7}$$

After this process, inductor L_1 charges cells B_2, B_3 and B_4 through the body diode of MOSFET $S_{1\mathrm{b}}$ to augment the charging currents of cells B_2, B_3 and B_4.

$$i_{\mathrm{B}_2} = i_{\mathrm{B}_3} = i_{\mathrm{B}_4} = I_{\mathrm{ch}} + i_{\mathrm{d1}} \tag{8}$$

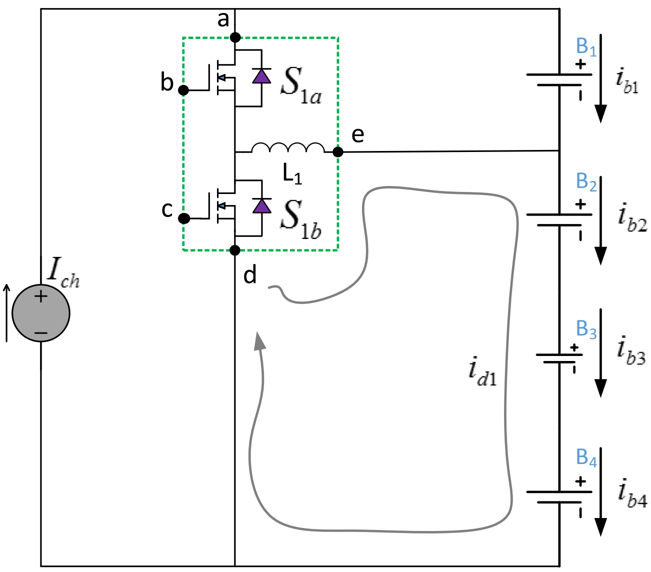

Figure 4. L_1 discharging schematic.

(2) Equalization principle for the discharging process or the suspended state after discharging

During discharging or in the suspended state after discharging, the equalization principle can be similarly divided into the following two stages. In the following, suppose the voltage of cell B_3 is lower than that of the other cells.

Stage 1: L_3 charges.

Figure 5 presents a schematic of the L_3 charging process. In this process, MOSFET S_{3a} is closed, cells B_1 and B_2 charge inductor L_3, and inductor L_3 stores the energy. Balancing sub-circuit S_3 absorbs the currents of cells B_1 and B_2 to increase their discharging current:

$$i_{B_1} = i_{B_2} = I_{dis} + i_{c3} \tag{9}$$

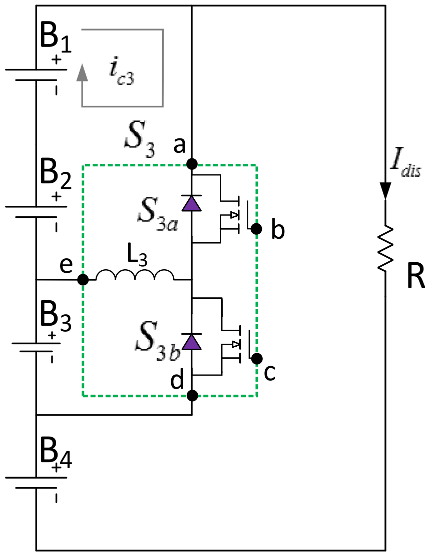

Figure 5. L_3 charging schematic.

Stage 2: L_3 discharges.

Figure 6 presents a schematic of the L_3 discharging process. In this process, MOSFET S_{3a} disconnects, and inductor L_3 charges cell B_3 by the body diode of MOSFET S_{3b} to decrease the discharging current of cell B_3:

$$i_{B_3} = I_{dis} - i_{d3} \tag{10}$$

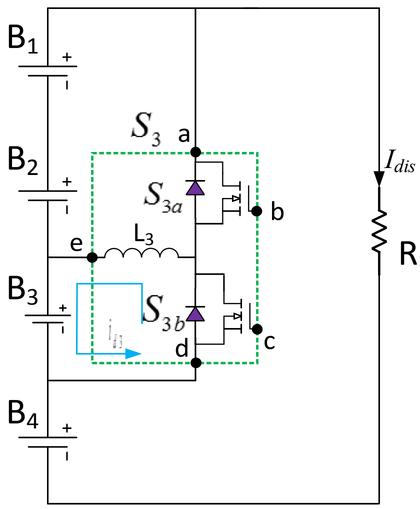

Figure 6. L_3 discharging schematic.

2.2.2. Equalization Principle for the Two Fluctuating Battery Parts

In the example of four single cells, suppose that the voltage in the upper half of the battery pack is greater than that in the lower half during charging or in the suspended state after charging and that the voltage values satisfy the working conditions of balancing sub-circuit *S*. Hence, the upper half of the battery requires discharge equalization, and the equalization process is divided into two stages as shown in Figure 7.

As shown in Figure 7a, when switch S_a is turned on, cells B_1 and B_2 charge inductor *L*. Then, as shown in Figure 7b, when switch S_a is disconnected, inductor *L* charges cells B_3 and B_4 by the body diode of S_b. Finally, the energy transfer from B_1 and B_2 to B_3 and B_4 is achieved.

Suppose that the voltage in the upper half of the battery pack is smaller than that in the lower half during discharging or in the suspended state after discharging and that the voltage values satisfy the working conditions of balancing sub-circuit *S*. The upper half then requires charging equalization, and the equalization process can be divided into two stages, as shown in Figure 8.

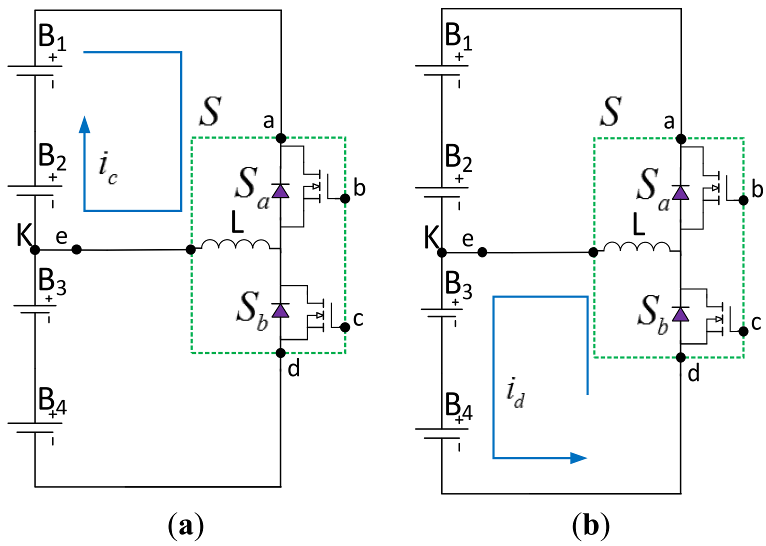

Figure 7. Working process of *L*. (**a**) *L* charging process; (**b**) *L* discharging process.

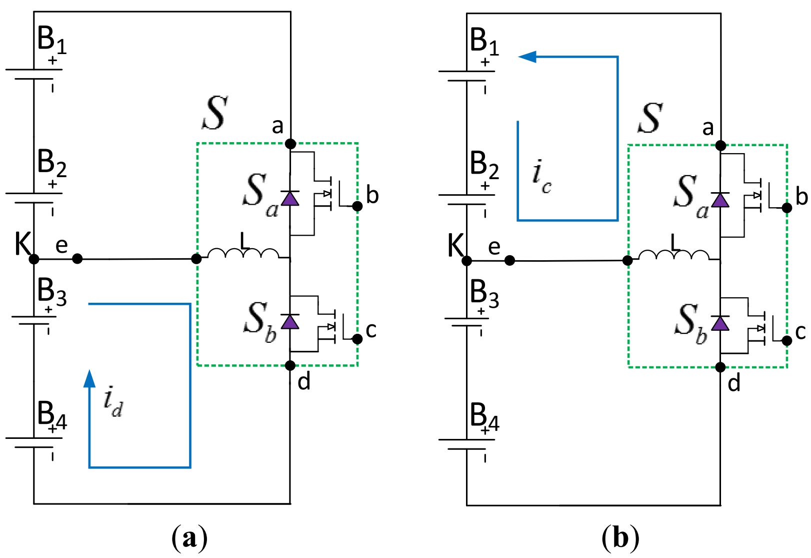

Figure 8. Working process of *L*. (**a**) *L* charging process; (**b**) *L* discharging process.

As shown in Figure 8a, when switch S_b is turned on, cells B_3 and B_4 charge inductor L. Then, as shown in Figure 8b, when switch S_b is disconnected, inductor L charges cells B_1 and B_2 by the body diode of S_a. Finally, the energy transfer from B_3 and B_4 to B_1 and B_2 is achieved.

3. Calculation of the Equalization Circuit Parameters

In this section, the fundamental parameters of the equalization circuit are calculated, including those for the charging process and the suspended state after charging and those for the discharging process and the suspended state after discharging.

3.1. Calculation of the Equalization Circuit Parameters for the Charging Process and the Suspended State after Charging

The resistance R_{on} in the equalization circuit is usually ignored during charging and in the suspended state after charging; when $i \leq k$ and the voltage of cell B_i is higher than that of the other cells, the control circuit manipulates balancing sub-circuit S_i to realize the discharge equalization of cell B_i.

The current passing through inductor L_i increases linearly when MOSFET S_{ia} is turned on. Meanwhile, inductor L_i stores the energy transmitted from cell B_i:

$$i_{L_i} = \frac{V_i \cdot t}{L} \quad (0 < t < D \cdot T) \tag{11}$$

where T represents the switching cycle, D represents the duty cycle, t represents the time, i_{Li} represents the inductor current of L_i, V_i represents the voltage of cell B_i, and L represents the inductance value of L_i.

The current passing through inductor L_i decreases linearly when MOSFET S_{ia} is turned off. Meanwhile, the inductor charges cells $B_{i+1}, B_{i+2}, \ldots, B_{n-1}, B_n$:

$$i_{Li} = I_P - \frac{\sum_{j=i+1}^{n} V_j \cdot t}{L} \quad (D \cdot T < t < T) \tag{12}$$

$$I_p = \frac{V_i \cdot D \cdot T}{L} \tag{13}$$

where I_p represents the peak current passing through inductor L_i and V_j represents the voltage of cell B_j.

The average charging current of cell B_i in balancing sub-circuit S_i decreases by I_{id} in one period:

$$I_{id} = \frac{1}{T} \cdot \frac{I_p \cdot D \cdot T}{2} = \frac{V_i \cdot D^2 \cdot T}{2L} \tag{14}$$

The average charging current of cells $B_{i+1}, B_{i+2}, \ldots, B_{n-1}, B_n$ in balancing sub-circuit S_i increases by I_{ioc} in one period:

$$I_{ioc} = \frac{1}{T} \cdot \frac{I_p \cdot T_f}{2} = \frac{V_i \cdot D \cdot T_f}{2L} \tag{15}$$

where T_f represents the time required for the current in the inductor to decrease from its maximum to zero.

When $i > k$, the control circuit accomplishes the discharge equalization of cell B_i by activating MOSFET $S_{i\mathrm{b}}$ in balancing sub-circuit S_i.

The current passing through inductor L_i increases linearly when MOSFET $S_{i\mathrm{b}}$ is turned on. Meanwhile, inductor L_i stores the energy transmitted from cell B_i:

$$i_{L_i} = \frac{V_i \cdot t}{L} \ (0 < t < D{\cdot}T) \tag{16}$$

The current passing through inductor L_i decreases linearly when MOSFET $S_{i\mathrm{b}}$ is turned off. Meanwhile, the inductor charges cells B_1, B_2,…, B_{i-1}:

$$i_{Li} = I_P - \frac{\sum_{j=1}^{i-1} V_j \cdot t}{L} \ (D{\cdot}T < t < T) \tag{17}$$

The average charging current of cell B_i in balancing sub-circuit S_i decreases by $I_{i\mathrm{d}}$ in one period:

$$I_{i\mathrm{d}} = \frac{1}{T} \cdot \frac{I_\mathrm{P} \cdot D \cdot T}{2} = \frac{V_i \cdot D^2 \cdot T}{2L} \tag{18}$$

The average charging current of cells B_1, B_2,…, B_{i-2}, B_{i-1} in balancing sub-circuit S_i increases by I_ioc in one period:

$$I_\mathrm{ioc} = \frac{1}{T} \cdot \frac{I_\mathrm{p} \cdot T_\mathrm{f}}{2} = \frac{V_i \cdot D \cdot T_\mathrm{f}}{2L} \tag{19}$$

where T_f represents the time required for the current in the inductor to decrease from its maximum to zero.

To ensure that the current passing through the inductor can return to zero within one period, $T_\mathrm{f} + D{\cdot}T \le T$ must be satisfied. The current in the inductor is in the discontinuous current mode (DCM) if $T_\mathrm{f} + D{\cdot}T < T$ and the critical continuous current mode (CCM) if $T_\mathrm{f} + D{\cdot}T = T$. Because the method for the parameter calculation for balancing sub-circuit S is the same as that for balancing sub-circuit S_i, it is omitted here.

3.2. Calculation of the Equalization Circuit Parameters for the Discharging Process and the Suspended State after Discharging

The resistance R_on in the equalization circuit is usually ignored within the discharge state. When $i \le k$, the control circuit manipulates balancing sub-circuit S_i to realize the charging equalization of cell B_i.

The current passing through inductor L_i increases linearly when MOSFET S_{ib} is turned on. Meanwhile, inductor L_i stores the energy transmitted from cells B_{i+1}, B_{i+2},…, B_{n-1}, B_n:

$$i_\mathrm{Li} = \frac{\sum_{j=i+1}^{n} V_j \cdot t}{L} \ (0 < t < D{\cdot}T) \tag{20}$$

The current passing through inductor L_i decreases linearly when MOSFET $S_{i\mathrm{b}}$ is turned off. Meanwhile, inductor L_i charges cell B_i:

$$i_{L_i} = I_p - \frac{V_i \cdot t}{L} \ (D{\cdot}T < t < T) \tag{21}$$

$$I_p = \frac{\sum_{j=i+1}^{n} V_j \bullet D \bullet T}{L} \tag{22}$$

where I_p represents the peak value of the current passing through inductor L_i, V_i represents the voltage of cell B_i, and V_j represents the voltage of cell B_j.

I_{ic} represents the average charging current of cell B_i per period manipulated by balancing sub-circuit S_i:

$$I_{ic} = \frac{1}{T} \cdot \frac{I_p \cdot T_f}{2} = \frac{\sum_{j=i+1}^{n} V_j \cdot D \cdot T_f}{2L} \tag{23}$$

where T_f represents the time required for the current in the inductor to decrease from its maximum to zero.

When $i > k$, the control circuit accomplishes the charging equalization of cell B_i by activating MOSFET S_{ia} in balancing sub-circuit S_i.

The current passing through inductor L_i increases linearly when MOSFET S_{ia} is turned on. Meanwhile, inductor L_i stores the energy transmitted from cells B_1, B_2,…, B_{i-2}, B_{i-1}:

$$i_{L_i} = \frac{\sum_{j=1}^{i-1} V_j \cdot t}{L} \ (0 < t < D{\cdot}T) \tag{24}$$

The current passing through inductor L_i decreases linearly when MOSFET S_{ia} is turned off. Meanwhile, the inductor charges cells B_i:

$$i_L = I_p - \frac{V_i \cdot t}{L} \ (D{\cdot}T < \mathrm{t} < T) \tag{25}$$

$$I_p = \frac{\sum_{j=1}^{i-1} V_j \cdot D \cdot T}{L} \tag{26}$$

where I_p represents the peak value of the current passing through inductor L_i, and V_i represents the voltage of cell B_i.

The average charging current value of cell B_i in balancing sub-circuit S_i increases by I_{ic} in one period:

$$I_{ic} = \frac{1}{T} \cdot \frac{I_p \cdot T_f}{2} = \frac{\sum_{j=1}^{i-1} V_j \cdot D \cdot T_f}{2L} \tag{27}$$

where T_f represents the time required for the current in the inductor to decrease from its maximum to zero.

To ensure that the current passing through the inductor can return to zero within one period, $T_f + D{\cdot}T \le T$ must be satisfied. The current in the inductor is in the DCM if $T_f + D{\cdot}T < T$ and the critical CCM if $T_f + D{\cdot}T = T$. Because the method for the parameter calculation of balancing sub-circuit S is the same as that for balancing sub-circuit S_i, it is omitted here.

4. Simulation Framework

The PSIM software was employed in the simulation, and the switching frequency was set to 10 kHz. To reduce the time required for equalization, capacitors (1F), which were regarded as ideal elements, were used as substitutes for the cells. It was assumed that the MOSFET and inductors were all ideal elements as well. Moreover, the influence of parasitic inductance and parasitic capacitance and the deviation generated by AD transfer were ignored. The topology of the circuit is presented in Figure 9. The active condition set for balancing sub-circuit S_i in the equalization control strategy during the charge process and in the suspended state after charging was $V_i = V_{\max} > V_{avg} + 10$ mV, $i = 1, 2, 3, 4$, $V_{avg} = (V_1 + V_2 + V_3 + V_4)/4$. The active condition set for balancing sub-circuit S was $\| (V_1 + V_2) | - | (V_3 + V_4) \| > 10$ mV. The active condition set for balancing sub-circuit S_i in the equalization control strategy during the discharge process and in the suspended state after discharging was $V_i = V_{\min} < V_{avg} - 10$ mV, $i = 1, 2, 3, 4$, $V_{avg} = (V_1 + V_2 + V_3 + V_4)/4$. The active condition set for balancing sub-circuit S was $\| (V_1 + V_2) | - | (V_3 + V_4) \| > 10$ mV.

Because the equalization principle of the charging state and the suspended state after charging are consistent, the equalization principle of the discharging state is the same as that of the suspended state after discharging. This section uses the suspended state after charging and the suspended state after discharging as examples. The equalization circuit topology is shown in Figure 9, and the equalization principles are validated as follows.

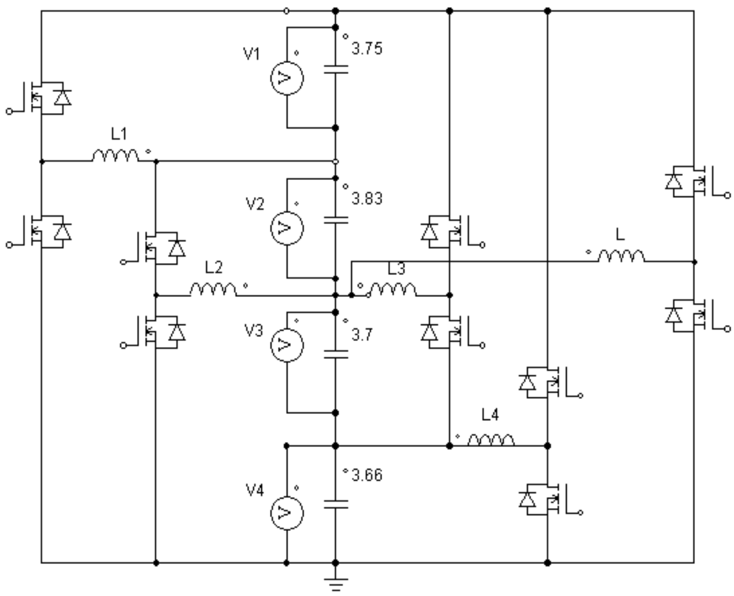

Figure 9. Simulation circuit diagram.

4.1. Simulation of Suspended State after Charging

Figure 10 presents the program flowchart of equalization during charging or in the suspended state after charging.

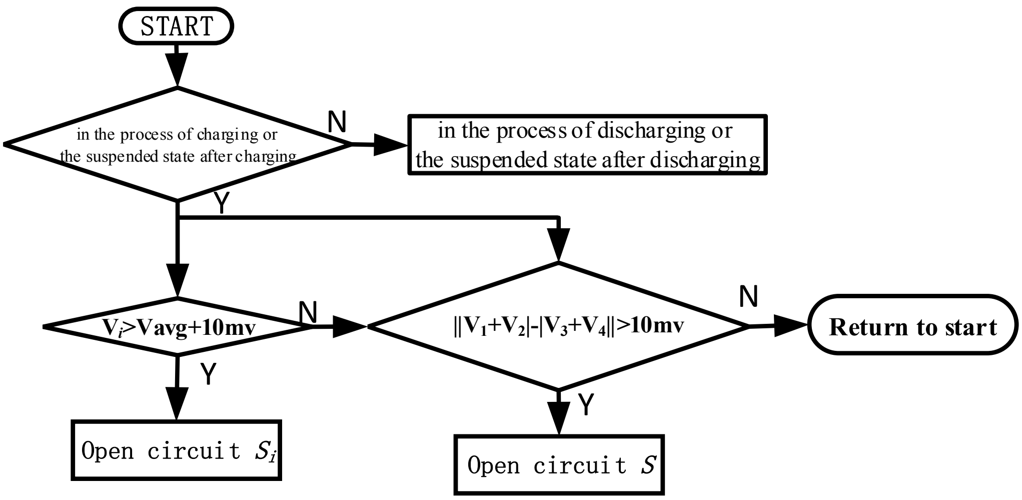

Figure 10. Program flowchart of equalization during charging or in the suspended state after charging.

When the battery pack is charging or in the suspended state after charging, the system will check the voltage of each cell to determine whether the working conditions of S_i and S are met. Balancing sub-circuit S_i will function under the condition in which $V_i = V_{max} > V_{avg} + 10$ mV, and balancing sub-circuit S will function under the condition in which $\| (V_1 + V_2) | - | (V_3 + V_4) \| > 10$ mV. The equalization will not stop unless neither the working condition for S nor that for S_i is achieved. In the simulation circuit topology shown in Figure 9, the voltage of cell B_2 is higher than those of the other cells. The simulation results are presented in Figure 11.

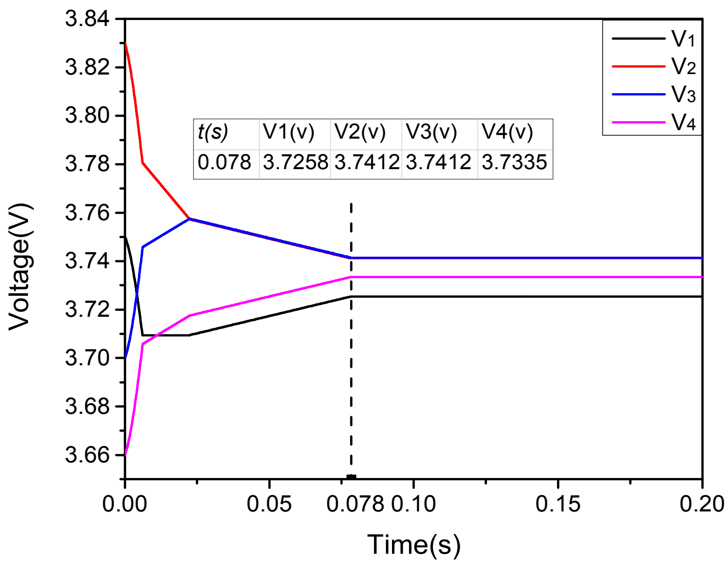

Figure 11. Terminal voltage of each cell.

Figure 11 illustrates that, when the equalization circuit starts to work, the voltage of each cell meets the working conditions of S and S_2; thus, balancing sub-circuits S and S_2 start to work, and the transfer of energy from B_2 to B_1, B_3 and B_4 is realized. All single-cell voltages converge at approximately 0.078 s, after which $V_i < V_{avg} + 10$ mV and $\| (V_1 + V_2) | - | (V_3 + V_4) \| < 10$ mV, the active conditions for S or S_i are not achieved, and the equalization goals are achieved.

4.2. Simulation of the Suspended State after Discharging

Figure 12 presents the program flowchart for equalization during discharging or in the suspended state after discharging.

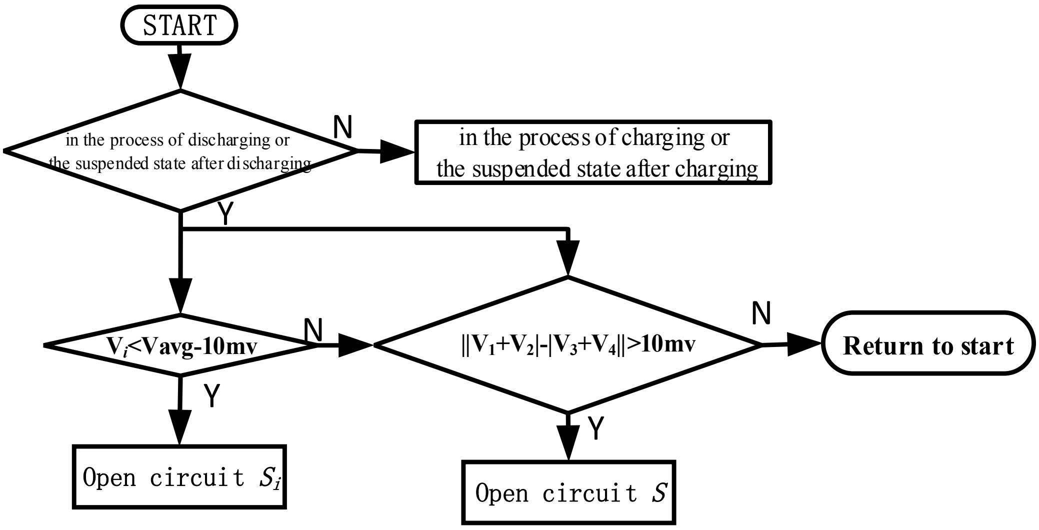

Figure 12. Program flowchart of equalization during discharging or in the suspended state after discharging.

When the battery pack is discharging or in the suspended state after discharging, the system will check the voltage of each cell to determine whether the working conditions of S_i and S are met. Balancing sub-circuit S_i will function under the condition in which $V_i = V_{\min} < V_{\text{avg}} - 10$ mV, and balancing sub-circuit S will function under the condition in which $\| (V_1 + V_2) \mid - \mid (V_3 + V_4) \| > 10$ mV. This equalization will not stop unless neither the working condition for S nor that for S_i is achieved. In the simulation of circuit topology shown in Figure 9, the voltage of cell B_4 is lower than those of the other cells. The simulation results are presented in Figure 13.

Figure 13 illustrates that, when the equalization circuit starts to work, the voltage of each cell meets the working conditions of S and S_4. Thus, balancing sub-circuits S and S_4 start to work, the transfer of energy from B_2 to B_1, B_3 and B_4 is realized, and the equalization will not stop unless neither the working condition for S nor that for S_i is achieved. As shown in the figure, all single-cell voltages converge at approximately 0.0049 s, after which $V_i > V_{\text{avg}} - 10$ mV, $\|(V_1 + V_2) \mid - \mid (V_3 + V_4)\| < 10$ mV, the active conditions for S or S_i are not qualified, and the equalization goals are achieved.

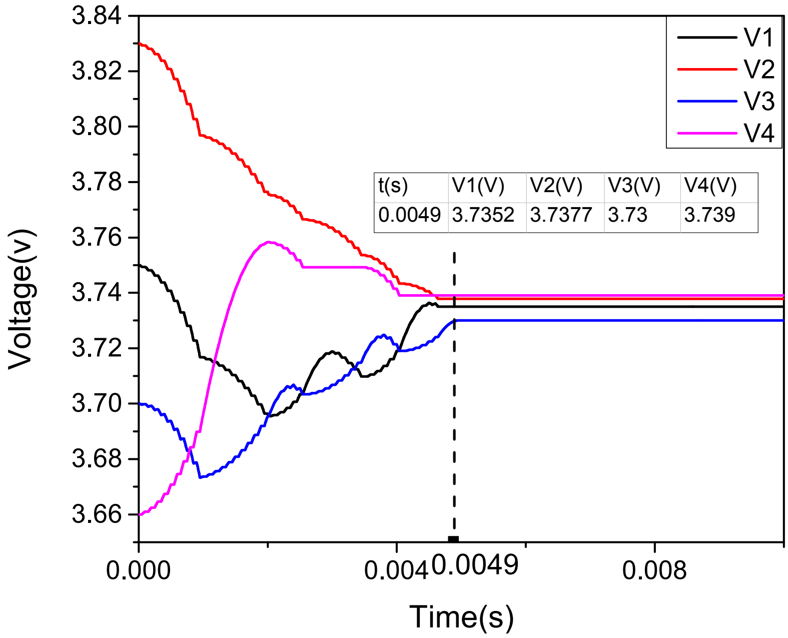

Figure 13. Terminal voltage of each cell.

5. Experimental Verification

Based on the above analysis, to further verify the effectiveness of the equalization circuit, an experiment was conducted using four three Ah $LiFePO_4$ batteries, with inductances of 330 μH and a switching frequency of 10 kHz. Figure 14 shows the experimental circuit.

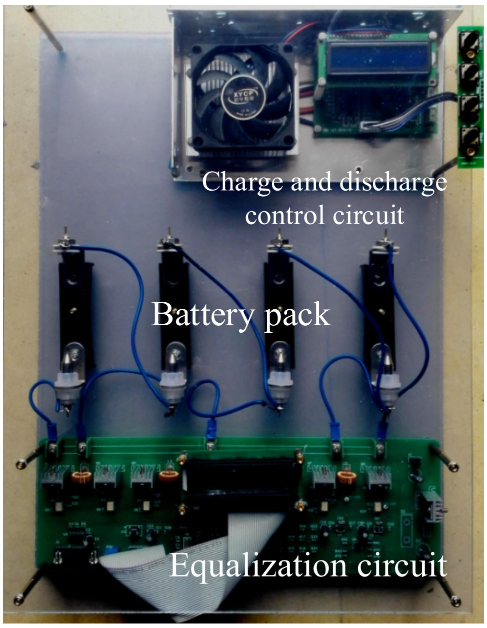

Figure 14. Experimental platform.

The role of the equalization circuit for the power battery was tested, including the charging process, the suspended state after charging, the discharging process, and the suspended state after discharging. To facilitate the analysis, the equalization current I_{eqi} was defined as the change in the average current of B_i after the action of balancing sub-circuits S_i and S; that is:

$$I_{\mathrm{eq}_i} = I_{\mathrm{B}_i}(t) - I_{\mathrm{B}_i}(0) \tag{28}$$

5.1. Experimental Results for the Charging Process and the Suspended State after Charging

The power battery charging current was set as I_{ch} = 500 mA, and the initial voltages of the cells were as shown in Table 1.

Table 1. Initial voltages of all cells for the charging process.

V_1	V_2	V_3	V_4	**Working Switch**
3.541	3.506	3.509	3.508	S_1, S
2.509	3.541	3.508	3.506	S_2, S
3.506	3.509	3.541	3.508	S_3, S
3.508	3.506	3.509	3.541	S_4, S

During charging, the average current values of Bi when balancing sub-circuits S_i and S were working are shown in Figure 15a. When voltage V1 was larger than the other cell voltages, all single-cell voltages before and after the work of the balancing sub-circuits are shown in Figure 15b. Figure 15a shows that $I_{\mathrm{eq}1}$ = −297 mA, $I_{\mathrm{eq}2}$ = −290 mA, $I_{\mathrm{eq}3}$ = −295 mA, and $I_{\mathrm{eq}4}$ = −294 mA when the power battery pack was charging with a 500 mA current. The equalization current $I_{\mathrm{eq}i}$ of the balancing sub-circuits reached up to 0.1 C. when sub-circuits S_i and S were working, they were able to reduce or even eliminate the charging current of the higher-voltage cell. Figure 15b shows that, after the work of the equalization circuit, all single-cell voltages converged.

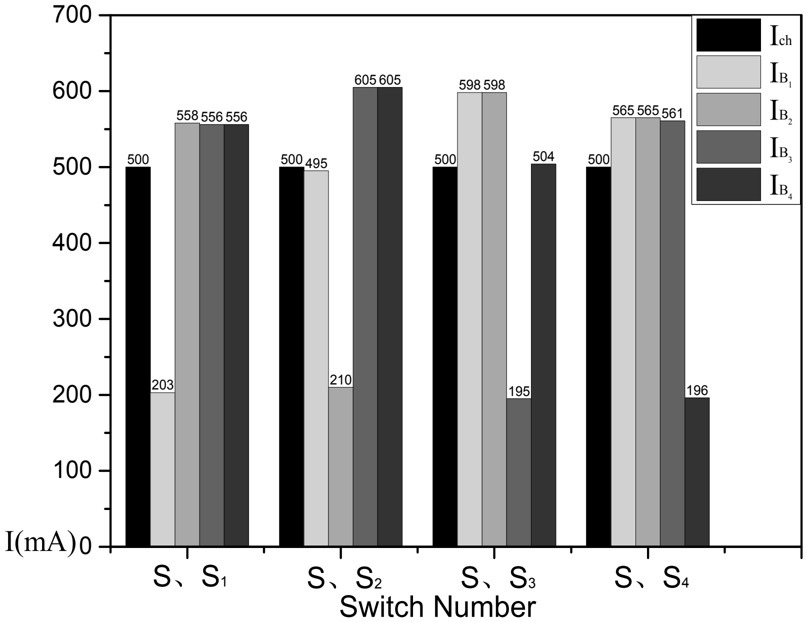

(**a**)

Figure 15. *Cont.*

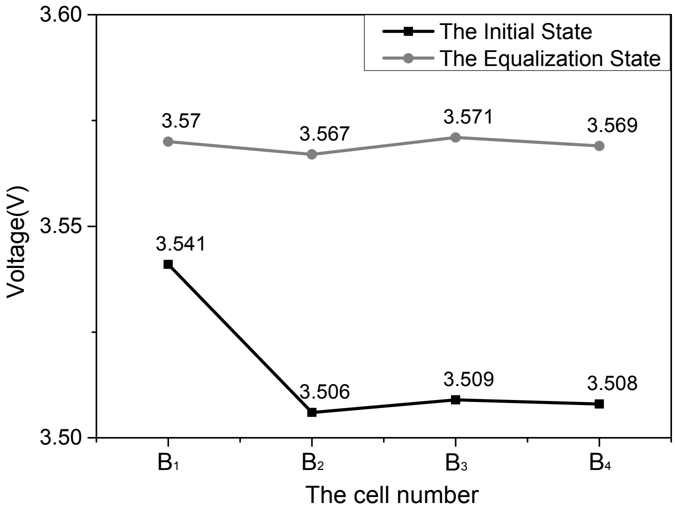

(**b**)

Figure 15. (**a**) Power battery pack charging current and single-cell currents; (**b**) Single-cell voltages before and after the work of the balancing sub-circuits.

In the suspended state after charging, the initial voltages of the four cells were as shown in Table 2.

Table 2. Initial voltages of all cells in the suspended state after charging.

V_1	V_2	V_3	V_4	**Working Switch**
3.54	3.509	3.508	3.51	S_1, S
2.51	3.54	3.509	3.508	S_2, S
3.506	3.509	3.54	3.508	S_3, S
3.509	3.508	3.51	3.54	S_4, S

The average current values of B_i when balancing sub-circuits S_i and S were working are shown in Figure 16a. When voltage V_3 was larger than the other cell voltages, all single-cell voltages before and after the work of the balancing sub-circuits are shown in Figure 16b.

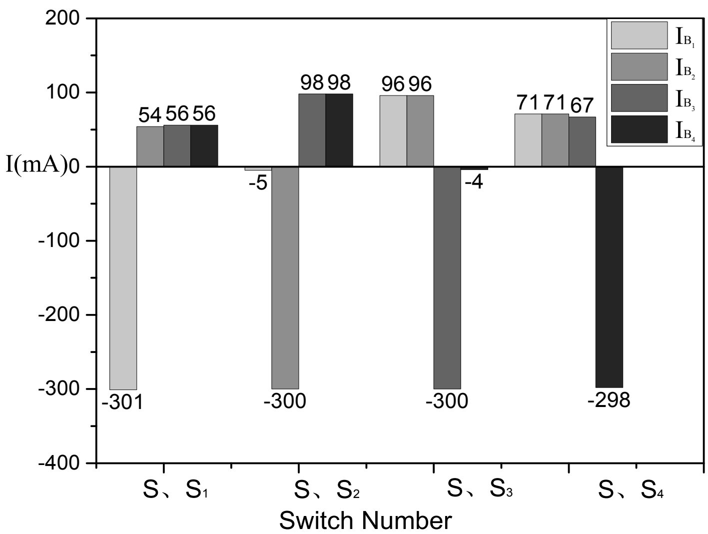

(**a**)

Figure 16. *Cont.*

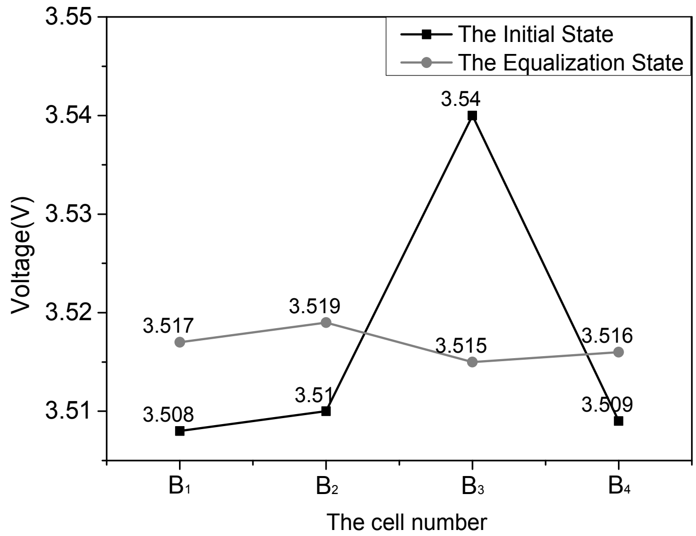

(**b**)

Figure 16. (**a**) Average current values of B_i during the work of sub-circuits S_i and S; (**b**) All single-cell voltages before and after the work of the balancing sub-circuits.

Figure 16a shows that $I_{eq1} = -301$ mA, $I_{eq2} = -300$ mA, $I_{eq3} = -300$ mA, $I_{eq4} = -298$ mA in the suspended state after charging. The equalization current I_{eqi} of the balancing sub-circuit reached up to 0.1 *C*. When sub-circuits S_i and S were working, they could transfer energy from the higher-energy cells to the lower-energy cells. Figure 16b shows that, after the operation of the equalization circuit, all single-cell voltages converged.

5.2. Experimental Results for the Discharging Process and the Suspended State after Discharging

The power battery discharging current was $I_{dis} = -500$ mA. During discharging, the initial voltages of the four cells were as shown in Table 3.

Table 3. Initial voltages of all cells for the discharging process.

V_1	V_2	V_3	V_4	**Working Switch**
2.84	2.924	2.921	2.923	S_1, S
2.923	2.84	2.924	2.921	S_2, S
2.921	2.923	2.84	2.924	S_3, S
2.924	2.921	2.923	2.84	S_4, S

The average current values of B_i when sub-circuits S_i and S were working are shown in Figure 17a. When voltage V_4 was lower than the other cell voltages, all single-cell voltages before and after the work of the balancing sub-circuit are shown in Figure 17b.

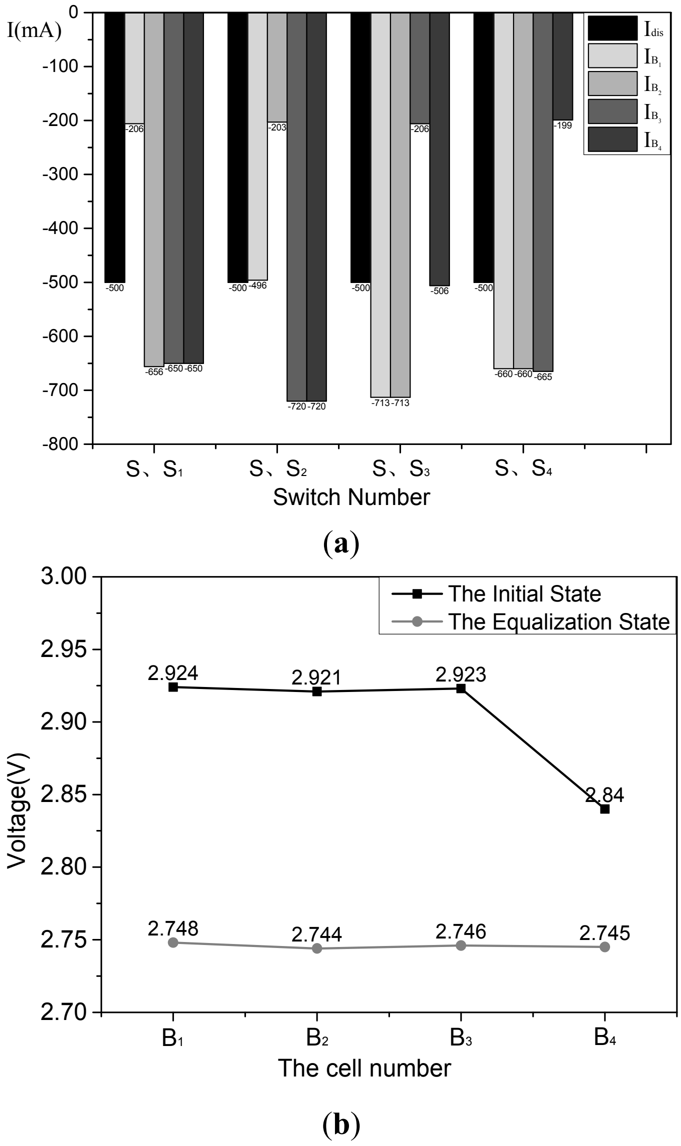

Figure 17. (**a**) Power battery pack discharging current and all single-cell currents; (**b**) All single-cell voltages before and after the work of the balancing sub-circuits.

Figure 17a shows that I_{eq1} = 294 mA, I_{eq2} = 297 mA, I_{eq3} = 294 mA, and I_{eq4} = 301 mA when the power battery pack was discharging at a current of 500 mA. The equalization current I_{eqi} of the balancing sub-circuit reached up to 0.1 C, showing that equalization circuit could reduce or even eliminate the discharge current of the cell with lower voltage. Figure 17b shows that, after the work of the equalization circuit, all single-cell voltages converged. In the suspended state after discharging, the initial voltages of the four cells were as shown in Table 4.

Table 4. Initial voltages of all cells in the suspended state after discharging.

V_1	V_2	V_3	V_4	Working Switch
2.823	2.886	2.885	2.884	S_1, S
2.884	2.823	2.886	2.885	S_2, S
2.885	2.884	2.823	2.886	S_3, S
2.886	2.885	2.884	2.823	S_4, S

The average current values of B_i when balancing sub-circuits S_i and S were working are shown in Figure 18a. When the voltage V_3 was lower than the other cell voltages, all single-cell voltages before and after the work of the balancing sub-circuits are shown in Figure 18b.

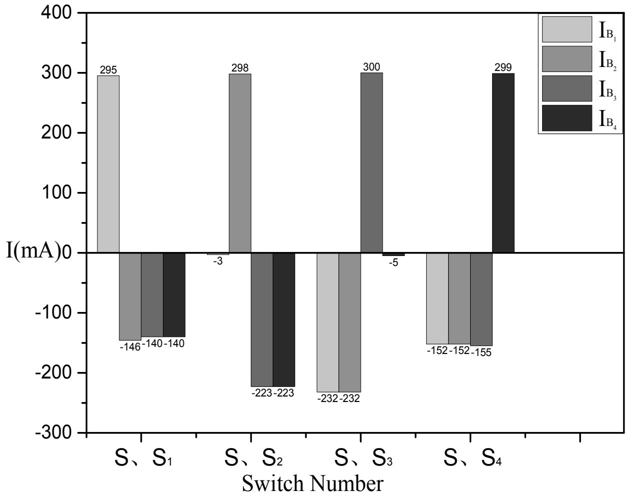

(**a**)

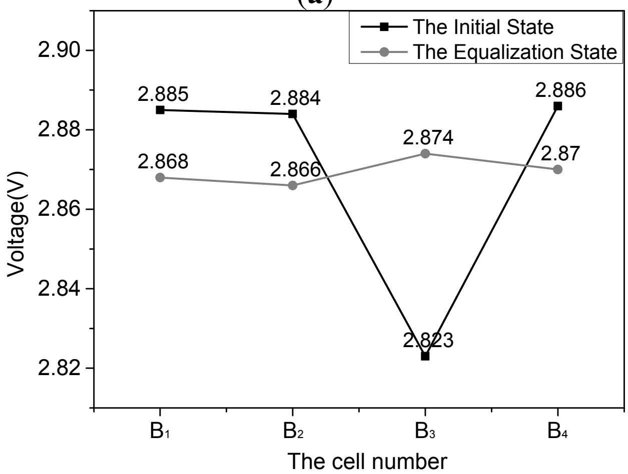

(**b**)

Figure 18. (**a**) Average current values of B_i during operation of sub-circuits S_i and S; (**b**) All single-cell voltages before and after the work of the balancing sub-circuits

Figure 18a shows that I_{eq1} = 295 mA, I_{eq2} = 298 mA, I_{eq3} = 300 mA, and I_{eq4} = 299 mA in the suspended state after discharging. The equalization current I_{eqi} of the balancing sub-circuit reached up to 0.1 C, showing that equalization circuit could transfer energy from higher-energy cells to lower-energy cells. Figure 18b shows that, after the work of the equalization circuit, all single-cell voltages converged.

6. Conclusions

Given the effects of variations in the lifecycle durations of series battery packs and the present state of equalization circuits, this paper proposes a novel voltage equalization circuit based on the buck-boost circuit. To verify the effectiveness of the proposed equalization circuit, a simulation model and experimental test platform were built. The simulation and experimental results show that the proposed equalization circuit can reduce the charging current of the higher-voltage cell during charging and decrease the discharging current of the lower-voltage cell during discharging. The circuit can discharge the higher-voltage cell in the suspended state after charging and charge the lower-voltage cell in the suspended state after discharging. This equalization circuit is characterized by high speed and large equalization currents. Future research will focus on using the single-cell state of charge as an index of inconsistency to achieve higher precision of the equalization circuit.

Acknowledgments

This work is supported by the National Natural Science Foundation of China (Grant No.51377058). I would like to express my deepest gratitude to my supervisor, Longyun Kang, who has provided me with valuable guidance at every stage of this paper-writing. I would also like to thank the anonymous reviewers for dedicating the time to review my paper despite their busy schedules.

Author Contributions

This research article has five authors. The circuit structure was designed by Xiangwei Guo and Longyun Kang. Xiangwei Guo and Zhizhen Huang conceived the research methods and control strategies. Xiangwei Guo, Yuan Yao and Huizhou Yang designed and performed the experiments. Longyun Kang contributed the experimental environment. Xiangwei Guo wrote the paper.

Conflicts of Interest

The authors declare no conflict of interest.

References

1. Scrosati, B.; Garche, J. Lithium batteries: Status, Prospects and Future. *J. Power Sour.* **2010**, *195*, 2419–2430.
2. Uno, M.; Tanaka, K. Single-switch multi-output charger using voltage multiplier for series-connected lithium-ion battery/super-capacitor equalization. *IEEE Trans. Ind. Electron.* **2013**, *60*, 3227–3239.
3. Kim, M.-Y.; Kim, C.-H.; Kim, J.-H.; Moon, G.-W. A chain structure of switched capacitor for improved cell balancing speed of lithium-ion batteries. *IEEE Trans. Ind. Electron.* **2014**, *61*, 3989–3999.
4. Lee, Y.S.; Cheng, M.W. Intelligent control battery equalization for series connected lithium-ion battery strings. *IEEE Trans. Ind. Electron.* **2005**, *52*, 1297–1307.
5. Yarlagadda, S.; Hartley, T.T.; Husain, I. A Battery Management System Using an Active Charge Equalization Technique Based on a DC/DC Converter Topology. In Proceedings of the 2011 IEEE Energy Conversion Congress and Exposition (ECCE), Phoenix, AZ, USA, 17–22 September 2011; pp. 1188–1195.
6. Lee, W.C.; Drury, D.; Mellor, P. Comparison of passive cell balancing and active cell balancing for automotive batteries. In Proceedings of the 2011 IEEE Vehicle Power and Propulsion Conference (VPPC), Chicago, IL, USA, 6–9 September 2011; pp. 1–7.
7. Danielson, C.; Borrelli, F.; Oliver, D.; Anderson, D.; Phillips, T. Constrained flow control in storage networks: Capacity maximization and balancing. *Automatica* **2013**, *49*, 2612–2621.

8. Daowd, M.; Omar, N.; van den Bossche, P.; van Mierlo, J. Passive and Active Battery Balancing comparison based on MATLAB Simulation. In Proceedings of the 2011 IEEE Vehicle Power and Propulsion Conference (VPPC), Chicago, IL, USA, 6–9 September 2011; pp. 1–7.
9. Kobzev, G.A. Switched-Capacitor Systems for Battery Equalization. Modern Techniques and Technology, Proceedings of the VI International Scientific and Practical Conference of Students, Post-graduates and Young Scientists, Tomsk, Russia, 28 February–3 March 2000; pp. 57–59.
10. Kim, T.; Park, N.; Kim, R. A high efficiency Zero Voltage-Zero Current Transition Converter for Battery Cell Equalization. In Proceedings of the 2012 Twenty-Seventh Annual IEEE Applied Power Electronics Conference and Exposition (APEC), Orlando, FL, USA, 5–9 February 2012; pp. 2590–2595.
11. Lu, X.; Qian, W.; Peng, F.Z. Modularized Buck-Boost + Cuk Converter for High Voltage Series Connected Battery Cells. In Proceedings of the 2012 Twenty-Seventh Annual IEEE Applied Power Electronics Conference and Exposition (APEC), Orlando, FL, USA, 5–9 February 2012; pp. 2272–2278.
12. Chen, W.-L.; Cheng, S.-R. Optimal charge equalisation control for seriesconnected Batteries. *IET Gener. Transm. Distrib.* **2013**, *8*, 843–854.
13. Hou, C.-H.; Yen, C.-T. A Battery Power Bank of Serial Battery Power Modules with Buck-Boost Converters. In Proceedings of the 2013 IEEE 10th International Conference on Power Electronics and Drive Systems (PEDS), Kitakyushu, Japan, 22–25 April 2013; pp. 211–216.
14. Ewanchuk, J.; Salmon, J. A modular balancing bridge for series connected voltage sources. *IEEE Trans. Ind. Electron.* **2014**, *29*, 4712–4722.
15. Kim, C.-H.; Kim, M.-Y. A modularized charge equalizer using a battery monitoring IC for series-connected li-ion battery strings in electric vehicles. *IEEE Trans. Ind. Electron.* **2013**, *28*, 3779–3787.
16. Phung, T.H.; Crebier, J.C.; Lembeye, Y. Voltage Balancing Converter Network for Series-connected Battery Stack. In Proceedings of the IECON 2012—38th Annual Conference on IEEE Industrial Electronics Society, Montreal, QC, Canada, 25–28 October 2012; pp. 3007–3013.
17. Lim, C.-S.; Lee, K.-J. A modularized equalization method based on magnetizing energy for a series-connected lithium-ion battery string. *IEEE Trans. Ind. Electron.* **2014**, *29*, 1791–1799.
18. Lotfi, N.; Fajri, P.; Novosad, S.; Savage, J.; Landers, R.G.; Ferdowsi, M. Development of an experimental testbed for research in lithium-ion battery management systems. *Energies* **2013**, *6*, 5231–5258.